



antioxidants

Supplementary Material

Polyester-based dendrimer nanoparticles combined with Etoposide have an improved cytotoxic and pro-oxidant effect on human neuroblastoma cells

Silvana Alfei,^{1,*§} Barbara Marengo,^{2§} and Cinzia Domenicotti^{2,*}

¹Department of Pharmacy, University of Genoa, Viale Cembrano, 4 I-16148 Genoa, Italy

²Department of Experimental Medicine - DIMES, Via Alberti L.B. 2 I- 16132 Genoa, Italy

§ Authors have equally contributed

*Corresponding Authors: cinzia.domenicotti@unige.it, alfei@difar.unige.it

Table of Contents

Figure S1: Structure of dendron intermediates synthesized to prepare **4**: D4BnA, D4BnOH, D5BnA and D5ACOOH

Section S1: Characterization of dendrimer **4**

*Table S1: Molecular Weight (MW) and significant physicochemical data of dendrimer **4***

*Copies of FTIR and NMR spectra of dendrimer **4***

*Figure S2: FTIR of dendrimer **4** (a), ¹H NMR of dendrimer **4** (b), ¹³C NMR and DEPT 135 of dendrimer **4** (c)*

Section S2: FTIR and NMR spectra of etoposide (ETO)

Figure S3: FTIR of ETO (a), ¹H NMR of ETO (b), ¹³C NMR of ETO (c)

Section S3: FTIR and NMR spectra of CPX **5**

*Figure S4: FTIR of CPX **5** (a), ¹H NMR of CPX **5** (b)*

Section S4: Comparison between FTIR and ¹H NMR spectra of ETO, dendrimer **4** and CPX **5**

*Figure S5: FTIR spectra of ETO (a), dendrimer **4** (b) and CPX **5** (c) with in evidence peaks of **4** (1), peaks of ETO (2) and of **5** (3)*

*Figure S6: ¹H-NMR spectra of ETO (a), dendrimer **4** (b) and CPX **5** (c)*

Section S5: Principal Components Analysis Results

Figure S7: Bi-plot and score plot on Components PC1 and PC2

Section S6: UV Spectrophotometric Analysis results

Table S2: Data of the calibration curve: $A_{average}$ and ETO standards $\mu\text{g/mL}$ concentrations. ETO predicted concentrations, residuals and ETO μM concentrations

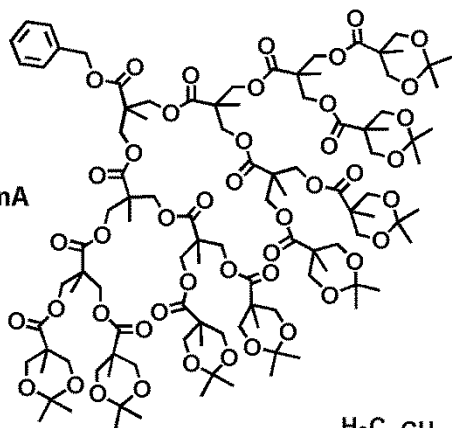
Figure S8: UV spectra of ETO dissolved in ACN/TDW 50:50 at the different concentrations used to build up the standard ETO calibration curve (a), standard ETO calibration curve (b), real ETO concentrations versus predicted ones (c), Absorbance (A) at $\lambda = 286 \text{ nm}$ versus standards ETO concentrations (μM)(d).

Section S7: DLS Results

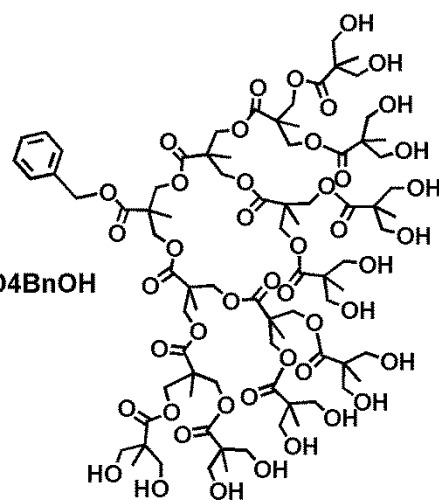
*Figure S9: Dynamic Light Scattering Analysis of CPX **5***

References

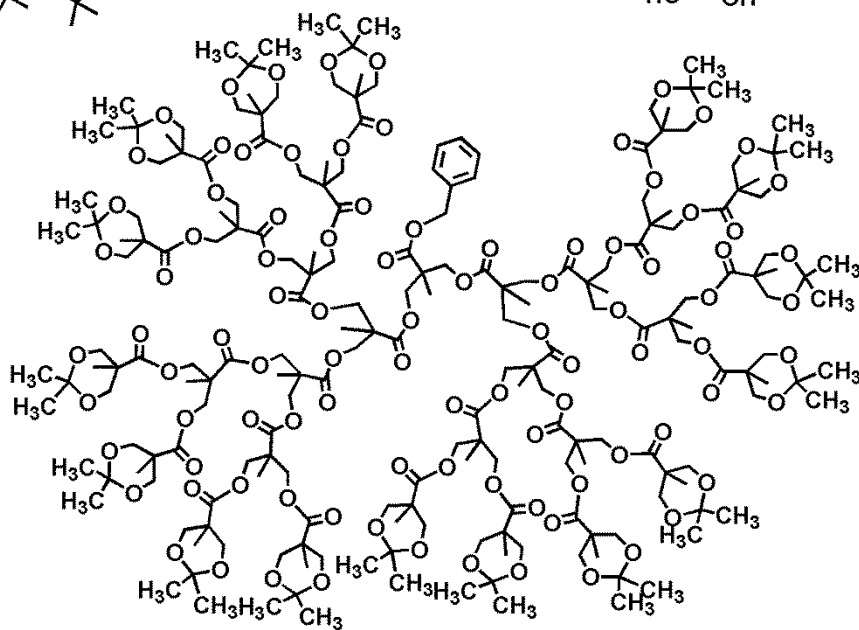
D4BnA



D4BnOH



D5BnA



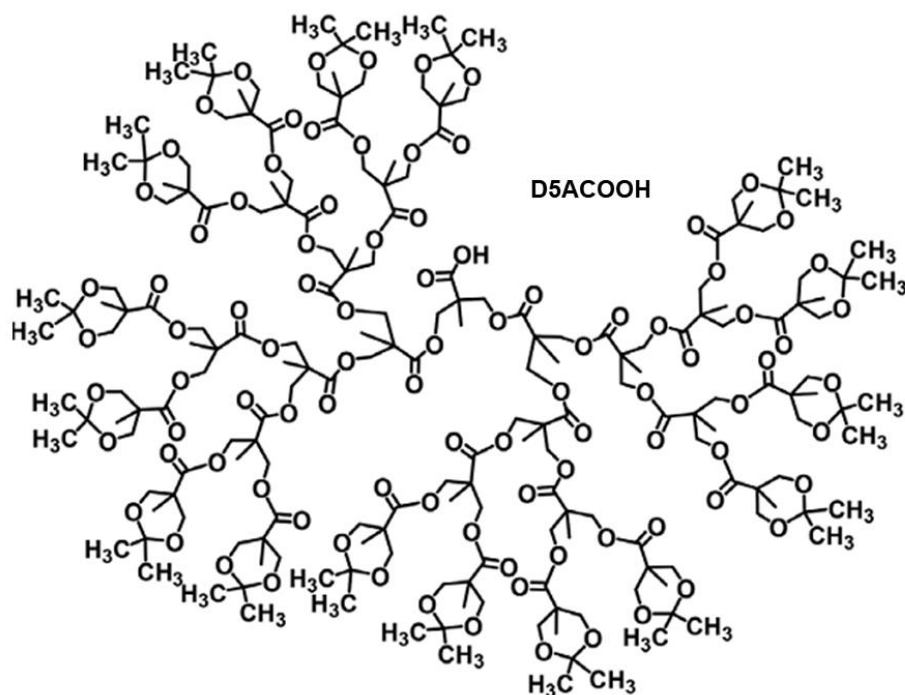


Figure S1. Structure of dendron intermediates achieved to synthesize **4**: D4BnA, D4BnOH, D5BnA and D5ACOOH

Section S1

Characterization data of dendrimer **4**

*FT-IR, NMR spectra data and Elemental analysis results of compound **4** [1]*

Dendrimer 4. FTIR (KBr, cm^{-1}): 3433 (OH), 2933, 1733 ($\text{C}=\text{O}$). ^1H NMR (300 MHz, $\text{DMSO}-d_6$), δ (ppm): 1.01, 1.16, 1.18, 1.23, 1.34 (five s signals, 186H, CH_3 of generations), 1.70 (m, 2H, CH_2 propandiol), 3.52 (dd, 128H, CH_2OH), 3.56 (partially overlapped signal, 2H, CH_2O propandiol), 3.98 (partially overlapped signal, 2H, CH_2O propandiol), 4.08-4.18 (m, 120H, CH_2O of four generations), 4.37 (br s, 64H, OH). ^{13}C NMR (75.5 MHz, $\text{DMSO}-d_6$) δ (ppm): 173.94, 171.73 ($\text{C}=\text{O}$), 64.27, 63.55 (CH_2O), 50.13 (quaternary C of fifth generation), 46.12 (other generation detectable quaternary C), 17.05, 16.61 (CH_3 of generations). Found: C, 51.71; H, 7.01. $\text{C}_{313}\text{H}_{504}\text{O}_{188}$ requires C, 51.67; H, 6.98%.

Table S1. Elemental Analysis and other physicochemical data of dendrimer **4** [1].

Compound	Formula	MW	Required (%)	Found (%)	Error (%)	Physical state
4	$\text{C}_{313}\text{H}_{504}\text{O}_{188}$ ¹	7275.24 ¹	C 51.67 H 6.98	C 51.71 H 7.01	C 0.04 H 0.03	Fluffy white hygroscopic solid

¹ Formula and MW of dendrimer **4** were estimated by ^1H NMR spectra and were confirmed by Elemental Analysis.

Copies of FT-IR and NMR spectra of dendrimer 4 [1]

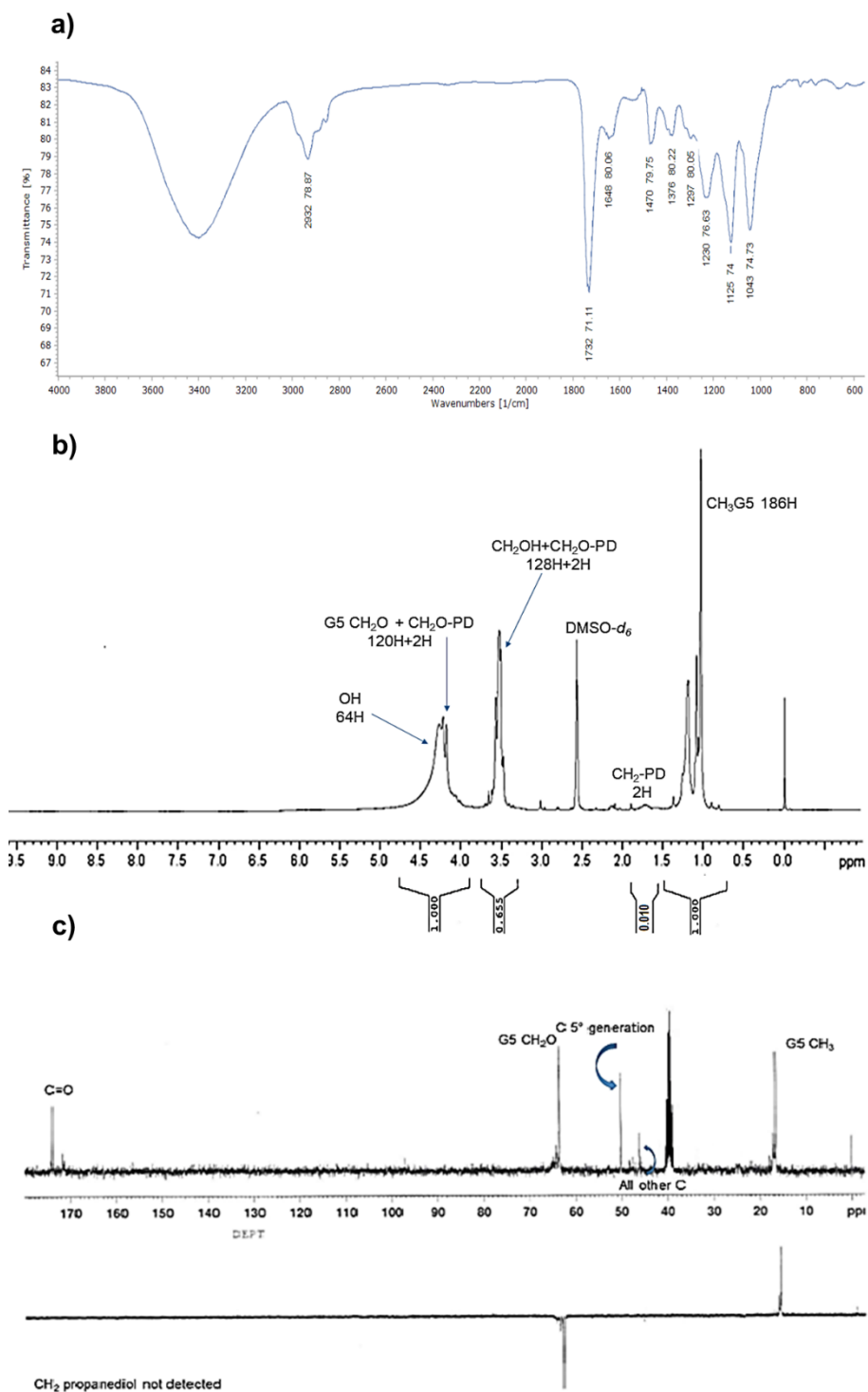


Figure S2. FTIR spectrum (KBr) (a), ¹H NMR spectrum (DMSO-*d*₆, 300 MHz) (b) and ¹³C NMR and DEPT 135 spectra (DMSO-*d*₆, 75.5 MHz) (c) of dendrimer 4.

Section S2

FTIR and NMR spectra of etoposide (ETO)

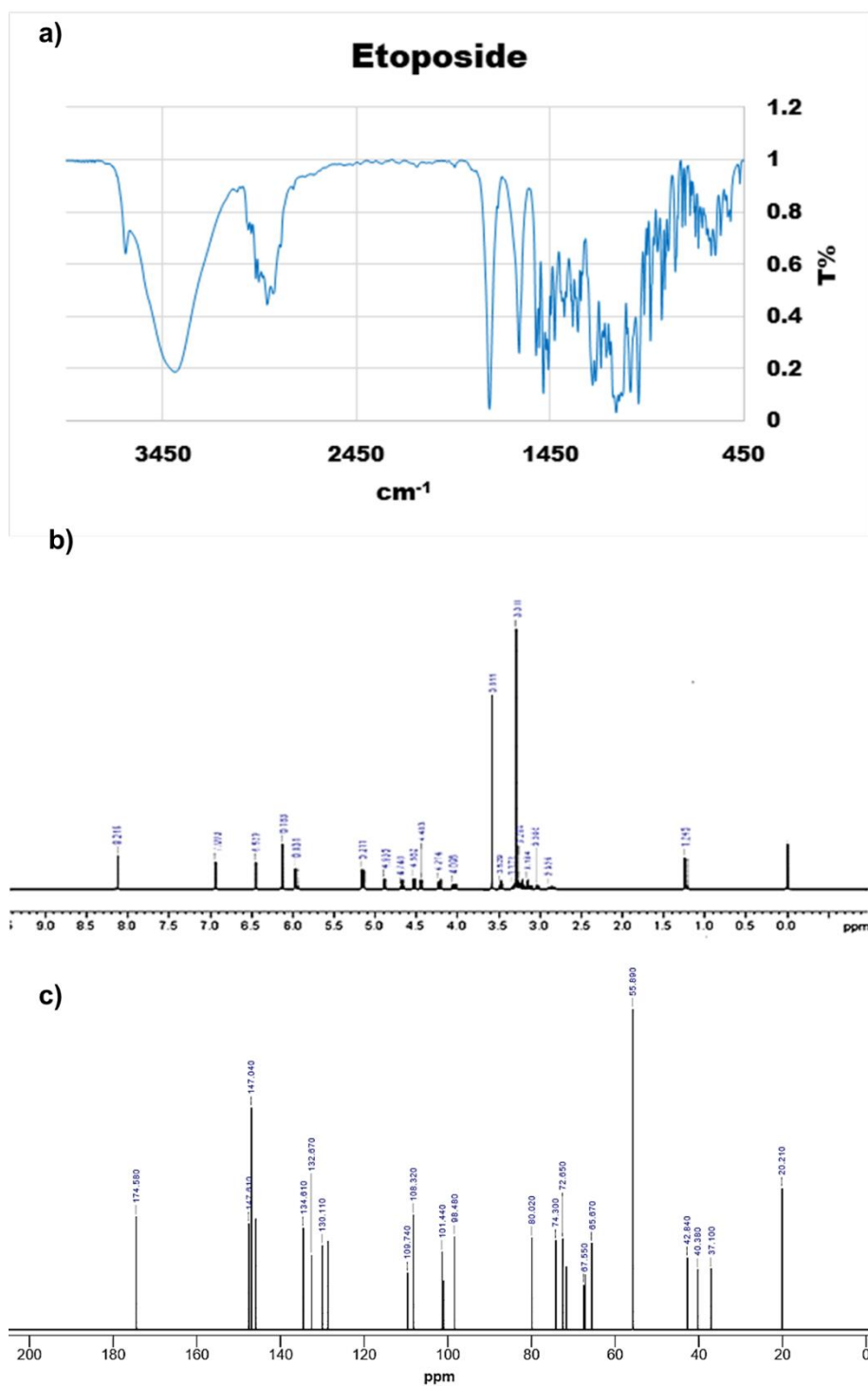


Figure S3. FTIR spectrum (KBr) (a), ^1H NMR spectrum (DMSO- d_6 , 400 MHz) (b) [2] and ^{13}C NMR spectrum (DMSO- d_6 , 100 MHz) (c) of ETO [2].

FTIR and NMR spectra of CPX 5

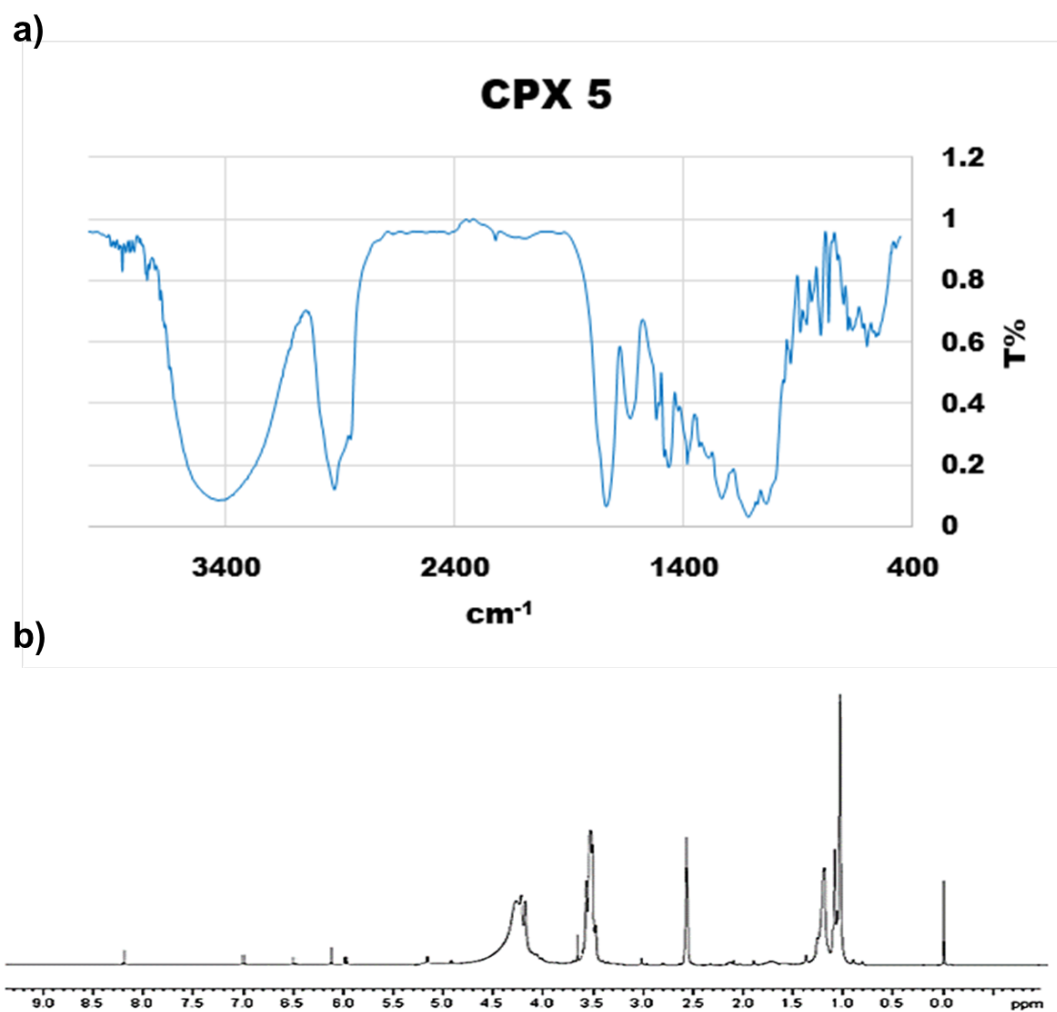


Figure S4. FTIR spectrum (KBr) (a) and ^1H NMR spectrum (DMSO- d_6 , 300 MHz) (b) of CPX 5.

Comparison between FTIR and NMR spectra of ETO, 4 and CPX 5

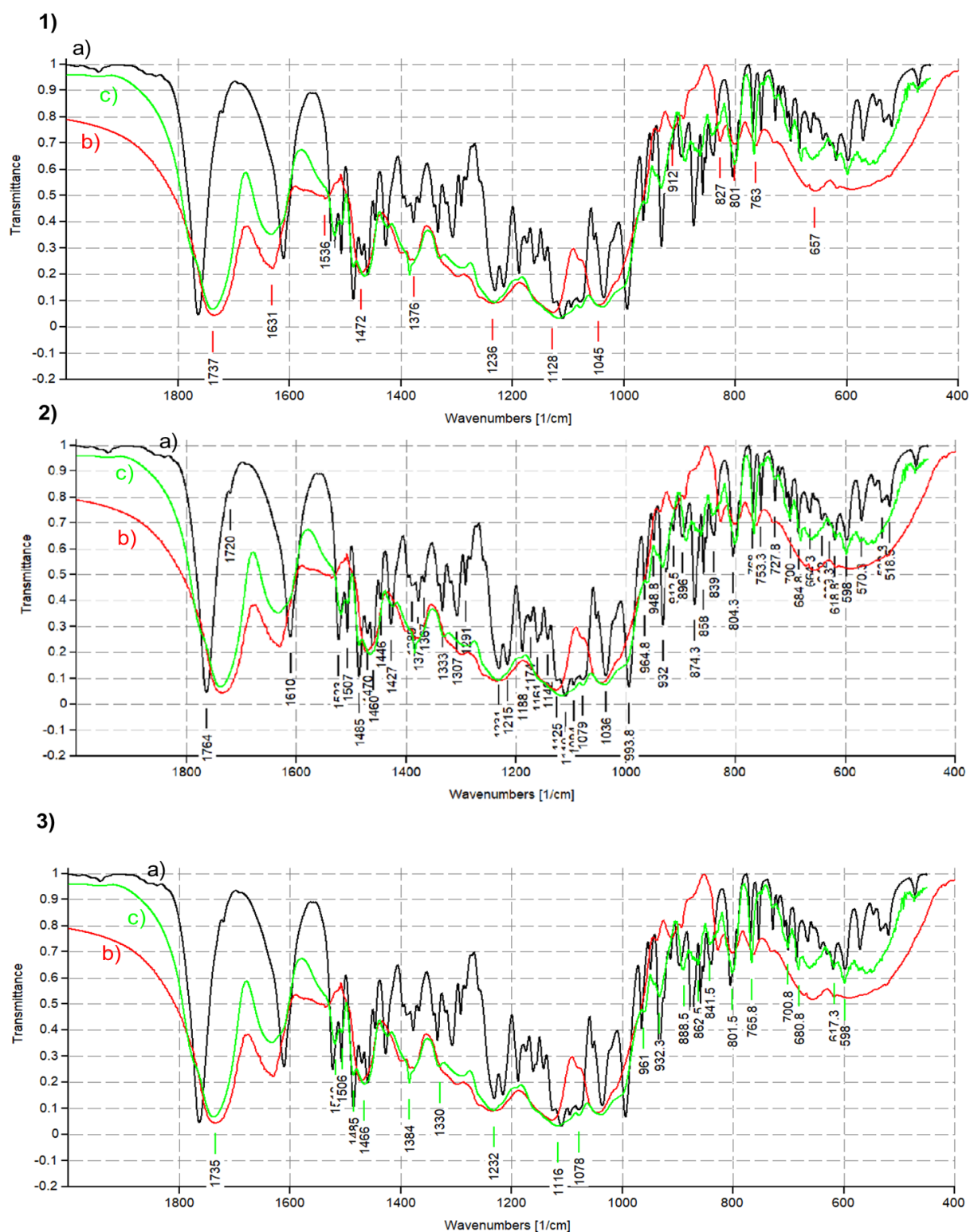


Figure S5. FTIR spectra of ETO (a), dendrimer 4 (b) and CPX 5 (c) with in evidence peaks of 4 (1), peaks of ETO (2) and peaks of 5 (3).

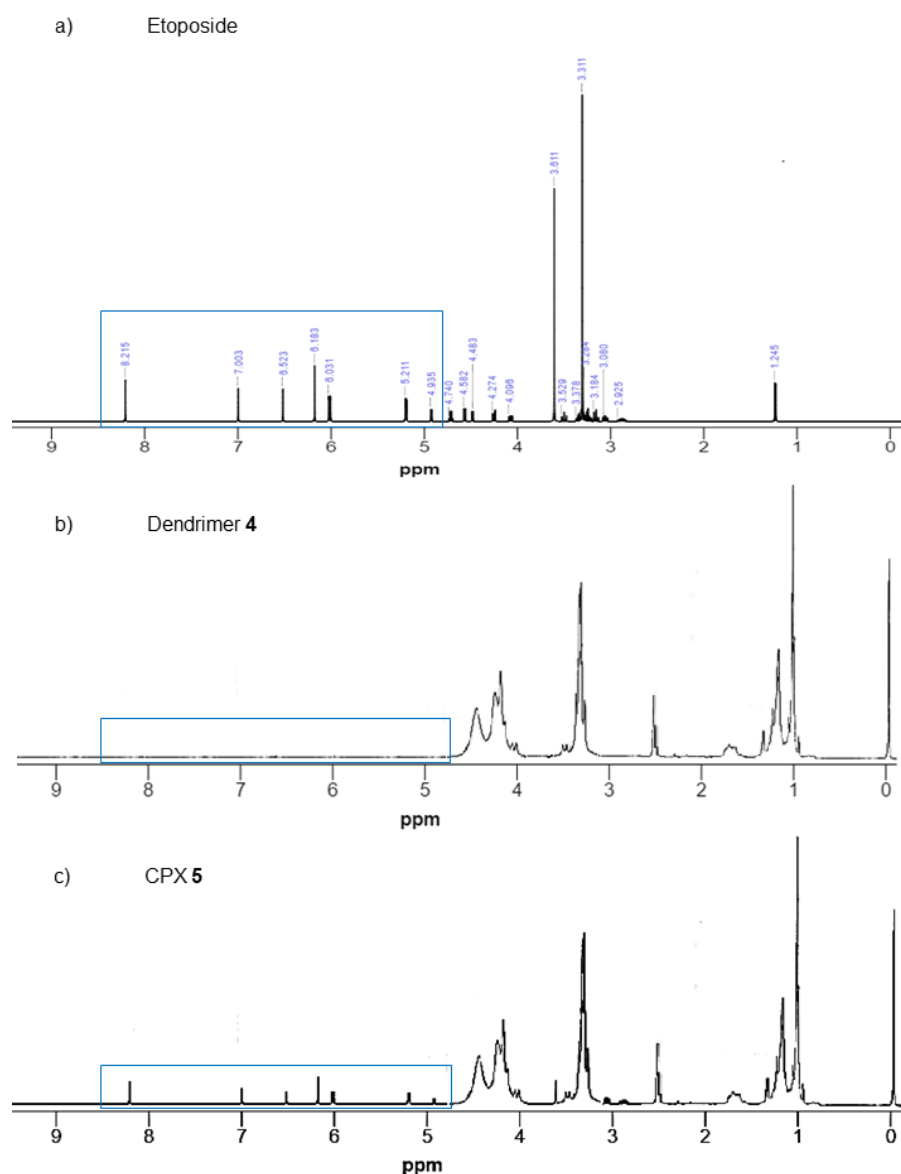


Figure S6. ^1H NMR spectra (DMSO- d_6) of (a) ETO (400 MHz) [2], (b) dendrimer **4** (300MHz) and (c) CPX **5** (300 MHz).

Section S5

Principal Component Analysis results

PCA is a chemometric tool extensively used to process FTIR spectral data obtained from very numerous samples population to put in comparison. In PCA, multi-dimensional data are reduced to a small number of new variables – principal components (PCs) – which are orthogonal linear combinations of the original ones that efficiently represent data variability in low dimensions [3]. Information carried out by PCs is expressed in terms of percentage of explained variance. By definition, PC1 has the largest % explained variance, followed by PC2, PC3 and so on [4]. Briefly, PCA is able to put in evidence similarities or differences among the samples under study by clustering or separating them within a square of two Components identified for being Principal Components (PC).

Variance explained by 5 components: 100%. % Variance explained by each component: 92.71, 6.26, 1.03, 0.00, 0.00



UV Spectrophotometric Analysis results

C_{ETO} ($\mu\text{g/mL}$)	$A_{\text{average}} \pm SD$	$C_{ETO\text{p}}$ ($\mu\text{g/mL}$)	Residuals	C_{ETO} (μM)
5.0	0.035 ± 0.020	4.8	-0.2	8.49
10.0	0.079 ± 0.013	10.1	+0.1	16.99
20.0	0.159 ± 0.018	19.9	-0.1	33.98
30.0	0.242 ± 0.024	30.0	0	50.97
40.0	0.321 ± 0.020	39.6	-0.4	67.96

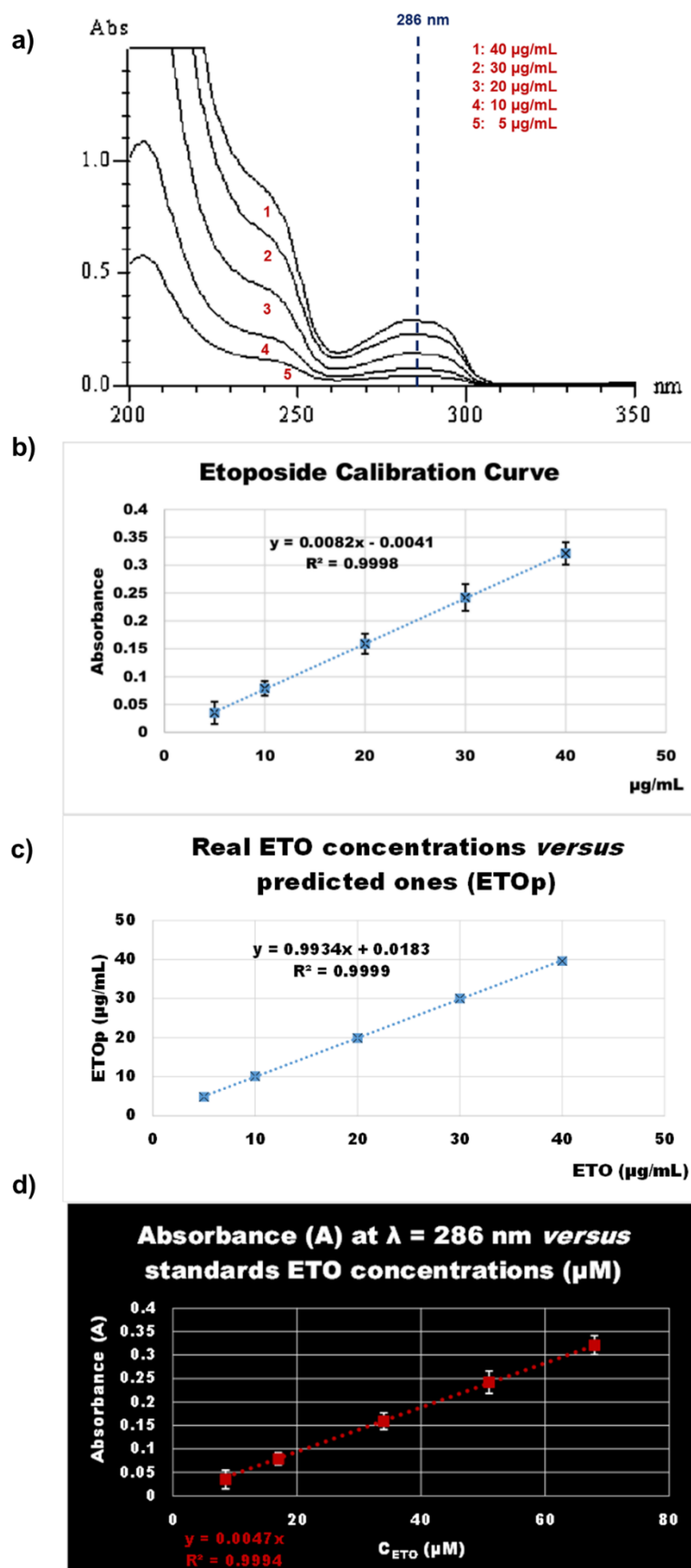


Figure S8. UV spectra of ETO dissolved in ACN/TDW 50:50 at the different concentrations used to build up the standard ETO calibration curve (a), standard ETO calibration curve (b), real ETO concentrations *versus* predicted ones (c), Absorbance (A) at $\lambda = 286$ nm *versus* standards ETO concentrations (μ M) (d).

Section S7

Dynamic Light Scattering Analysis

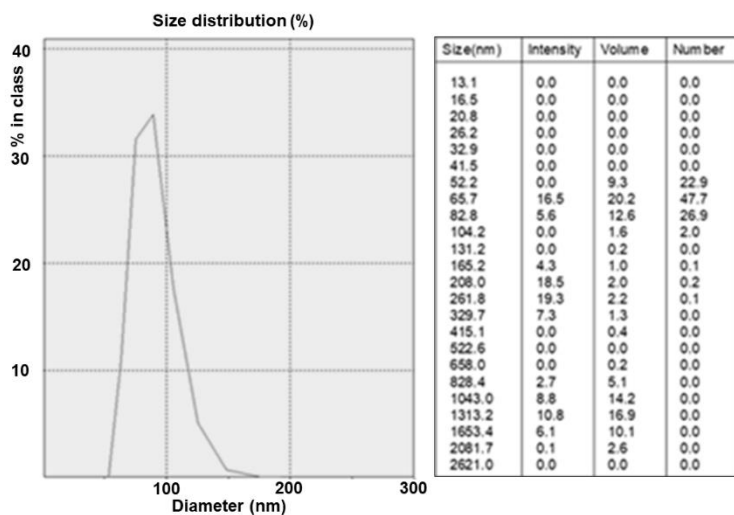


Figure S9. Dynamic Light Scattering Analysis of CPX 5

References

- [1] Alfei, S.; Catena, S.; Turrini, F. Biodegradable and biocompatible spherical dendrimer nanoparticles with a gallic acid shell, as double-acting, high performant antioxidant device to fight diseases from "oxidative stress", *Drug Deliv. Transl. Res.* **2019**. <https://doi.org/10.1007/s13346-019-00681-8>.
- [2] Spectral Database for Organic Compounds (SDBS): https://sdb.sdb.aist.go.jp/sdb/cgi-bin/direct_frame_top.cgi (latest access, 24 November 2019).
- [3] Jolliffe, I.T.; Cadima, J. Principal component analysis: a review and recent developments. *Philos. Trans. A Math. Phys. Eng. Sci.* **2016**, *374*, 20150202.
- [4] Alfei, S.; Oliveri, P.; Malegori, C. Assessment of the Efficiency of a Nanospherical Gallic Acid Dendrimer for Long-Term Preservation of Essential Oils: An Integrated Chemometric-Assisted FTIR Study. *ChemistrySelect* **2019**, *4*, 8891 -8901.